

Two Routes to Vesicle Formation: Metal–Ligand Complexation and Ionic Interactions

Jingzheng Wang,[†] Aixin Song,[‡] Xiangfeng Jia,[†] Jingcheng Hao,^{*,†,‡} Weimin Liu,^{*,‡} and Heinz Hoffmann[§]

Key Laboratory of Colloid and Interface Chemistry (Shandong University), Ministry of Education, Jinan 250100, P. R. China, State Key Laboratory of Solid Lubrication, Lanzhou Institute of Chemical Physics, Chinese Academy of Sciences, Lanzhou 730000, P. R. China, and Universität Bayreuth, Bayreuther Zentrum für Kolloide und Grenzflächen, D-95446 Bayreuth, Germany

Received: December 2, 2004; In Final Form: April 19, 2005

Two routes to vesicle formation were designed to prepare uni- and multilamellar vesicles in salt-free aqueous solutions of surfactants. The formation of a surfactant complex between a double-chain anionic surfactant with a divalent-metal ion as the counterion and a single-chain zwitterionic surfactant with the polar group of amine-oxide group is described for the first time as a powerful driving force for vesicle-phases constructed from salt-free mixtures of aqueous surfactant solutions. As a typical example, a Zn^{2+} -induced charged complex fluid, vesicle-phase has been studied in aqueous mixtures of tetradecyldimethylamine oxide (C_{14}DMAO) and zinc 2,2-dihydroperfluorooctanoate [$\text{Zn}(\text{OOCCH}_2\text{C}_6\text{F}_{13})_2$]. This ionically charged vesicle-phase formed due to surfactant complexation has interesting rheological properties and is not shielded by excess salts because there are no counterions in the solution. Such a vesicle-phase of surfactant complex is important for many applications; for example, the vesicle-phase was further used to produce in situ the vesicle-phase of the salt-free cationic/anionic (catanionic) surfactants, $\text{C}_{14}\text{DMAOH}^+-\text{OOCCH}_2\text{C}_6\text{F}_{13}$. The salt-free catanionic vesicle-phase could be produced through injecting H_2S gas into the $\text{C}_{14}\text{DMAO}/\text{Zn}(\text{OOCCH}_2\text{C}_6\text{F}_{13})_2$ vesicle-phase, because the zwitterionic surfactant C_{14}DMAO can be charged by the H^+ released from H_2S to become a cationic surfactant and Zn^{2+} was precipitated as ZnS . After the ZnS precipitates were removed from $\text{C}_{14}\text{DMAO}/\text{Zn}(\text{OOCCH}_2\text{C}_6\text{F}_{13})_2$ solutions, the final mixed solution does not contain excess salts as do other cationic/anionic surfactant systems. Both the $\text{C}_{14}\text{DMAO}-\text{Zn}(\text{OOCCH}_2\text{C}_6\text{F}_{13})_2$ complex and the resulting catanionic $\text{C}_{14}\text{DMAOH}^+-\text{OOCCH}_2\text{C}_6\text{F}_{13}$ solution are birefringent $\text{L}\alpha$ -phase solutions that consist of uni- and multilamellar vesicles. Ring-shaped semiconductor ZnS materials with encapsulated ZnS precipitates and regular spherical ZnS particles were prepared, which resulted in a transition from vesicles composed of metal–ligand complexes to vesicles held together by ionic interactions in the salt-free aqueous systems. This strategy should provide a new method to prepare inorganic materials. The present routes to form vesicles solve a problem: how to prepare nanomaterials using surfactant self-assembly, with structure controlled not by the growing material, but by the phase behavior of the surfactants.

Introduction

The rapidly growing research in controlling the size and morphology of nanostructured materials has created an increasing demand for supramolecular self-assemblies used as organized templates, which should be easily constructed in a highly reproducible way and with a perfect control of the organized structures. A number of different organized assemblies, such as spherical,¹ rodlike or wormlike,² and disklike micelles,³ flat lamellar bilayers,^{1a,4} closed uni- and multilamellar vesicles,⁵ and sponge structures with branched bicontinuous tubes,⁶ have all been recently used to produce advanced nanostructured materials.⁷ The main driving force for constructing the organized assemblies of amphiphiles arises from weak van der Waals, hydrophobic, hydrogen-bonding, and screened electrostatic interactions, etc.⁸ In recent years, hydrogen bonding⁹ and metal–ligand complexes¹⁰ have been introduced as noncovalent

interactions for the engineering of supramolecular assemblies. Three typical noncovalent interactions are depicted in Figure 1: ionic, hydrogen bonding, and metal–ligand complexes.

The use of ionic interactions to form supramolecular assemblies (see Figure 1a) is exemplified in cationic–anionic surfactant mixtures (i.e., so-called catanionic mixed solutions). The catanionic mixed solutions are the fascinating subject of extensive recent investigations¹¹ because the mixtures of oppositely charged surfactants exhibit novel solution and interface properties, i.e., the aggregation in aqueous mixtures of cationic and anionic surfactants occurs at considerably lower concentrations than the critical micelle concentration (cmc) of each individual surfactant. The coadjustment of electrostatic effects and surfactant molecular geometry allows a rich diversity of phase behavior. The phase behavior and microstructures of many catanionic mixtures have been explored in the last 15 years after spontaneous vesicles were prepared in 1989.¹² Particular self-assembled aggregates and their properties have been investigated such as the equilibrium among bilayer cylinders, spheres, and disks,^{3,13} and new self-assembled shapes such as regular hollow icosahedra.¹⁴ Vesicles^{5,12,15} in catanionic surfactant solutions have very noticeable aspects. A recent report has been described

* Corresponding author: E-mail: jhao@sdu.edu.cn, Phone: +86-531-8366074(o), Fax: +86-531-8564464(o).

[†] Shandong University.

[‡] Lanzhou Institute.

[§] Universität Bayreuth.

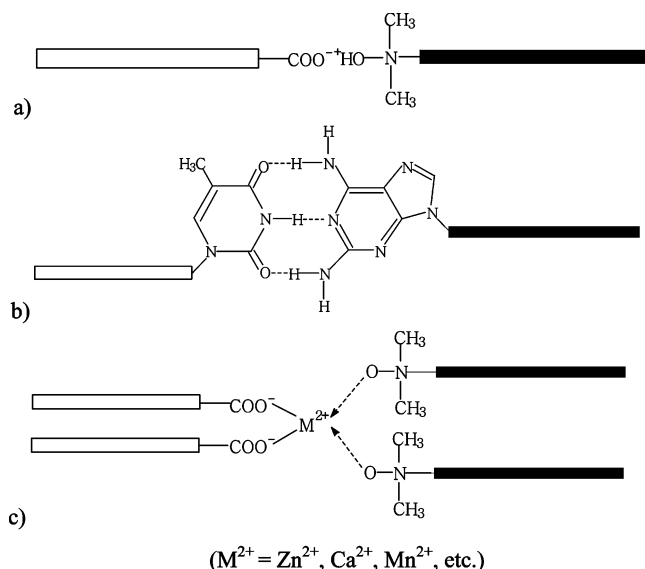


Figure 1. Typical bonding interactions to supramolecular multichain amphiphiles. (a) Ionic interactions between single-chained surfactants bearing oppositely charged end-groups. (b) Recognition hydrogen bonding between purine- and thymine-functionalized amphiphiles. (c) Metal-ligand interaction in asymmetrical metal ionic-surfactant and zwitterionic surfactant complexes.

on the origins of stability of spontaneous vesicles formed in two catanionic surfactant systems of cetyltrimethylammonium bromide (CTAB)/sodium octyl sulfonate (SOS) and CTAB/sodium perfluorooctanoate (CF_7).¹⁶ The magnitude of the ionic interactions in catanionic surfactants can be quite high and is easily modulated through the dielectric constant. However, these strong ionic interactions are neither directional nor selective, which limits the use of mixtures of catanionic surfactants as novel templates for preparing nanoscale materials.

Hydrogen bonded assemblies, especially in macromolecular architectures, have been recently prepared.⁹ This work received significant attention due to the thermoreversible and molecular recognition features of the resulting self-assemblies. Complementary multiply hydrogen bonding units are good candidates to construct supramolecular hydrogen-bonded architectures. Nature uses this strategy in the heterocyclic base pairing between adenine, guanine, thymine, uracil, and tyrosine in DNA and RNA. Nevertheless, to date, there have been few reports of hydrogen-bonded self-assemblies of traditional surfactants in aqueous solutions because the strength of the hydrogen bonds is rather weak compared with ionic or metal-ligand interactions. Organized supramolecular architectures of low molecular weight amphiphiles such as the monoalkyloxamide amphiphiles formed by complementary hydrogen bonding were reported by Liang's and Rotello's group.¹⁷ The self-complementary intermolecular hydrogen bond networks are formed between an oxamido group and its neighbors. However, this study was focused on the formation of ordered bilayer aggregates at interfaces, and little was reported about aggregates in the bulk solution.

Metal-ligand complexation can be used to form supramolecular links as illustrated in Figure 1c. This strategy has been previously successfully used to produce asymmetric bis-2,2':6',2''-terpyridine-ruthenium(II) complexes with various organic compounds.¹⁸ Metal-ligand complexes have only recently been investigated in traditional surfactant systems. Recently, we presented a short report on vesicle formation by Zn^{2+} -ligand complexes from surfactant mixtures of C_{14}DMAO and $\text{Zn}(\text{OOCCH}_2\text{C}_6\text{F}_{13})_2$.^{16b} In the C_{14}DMAO and $\text{Zn}(\text{OOCCH}_2\text{C}_6\text{F}_{13})_2$

aqueous mixtures, Zn^{2+} is the central ion forming charged membranes without counterions in solution.

In the present article, we present in detail the total preparation of a charged surfactant vesicle-phase without any cosurfactants. The ionic charges are not shielded because the solutions are salt-free in the $\text{C}_{14}\text{DMAO}/\text{Zn}(\text{OOCCH}_2\text{C}_6\text{F}_{13})_2$ system. The formation of the charged vesicle-phase was induced by the heavy metal ion, Zn^{2+} . Metal-ligand complexes play an important role in producing salt-free vesicles. We observed the phase behavior of $0.10 \text{ mol} \cdot \text{dm}^{-3}$ C_{14}DMAO with increasing amounts of $\text{Zn}(\text{OOCCH}_2\text{C}_6\text{F}_{13})_2$ in aqueous solution. The birefringent $\text{L}\alpha$ -phase with uni- and multilamellar vesicles was demonstrated by freeze-fracture transmission electron microscopy (FF-TEM). Ring-shaped semiconductor ZnS materials with encapsulated ZnS precipitates and regular spherical ZnS particles were prepared by flowing H_2S gas at room temperature into birefringent solutions of vesicle-phase containing C_{14}DMAO and $\text{Zn}(\text{OOCCH}_2\text{C}_6\text{F}_{13})_2$. Vesicle formation may be the result of complexation between Zn^{2+} and the amine-oxide group of $\text{C}_{14}\text{-DMAO}$. When H_2S gas is injected into the vesicle-phase, Zn^{2+} is precipitated by H_2S , while the zwitterionic surfactant $\text{C}_{14}\text{-DMAO}$ is charged by the H^+ released by H_2S to cationic surfactant producing the combined cationic/anionic surfactant system $\text{C}_{14}\text{DMAOH}^+-\text{OOCCH}_2\text{C}_6\text{F}_{13}$. After removal of ZnS precipitates, the catanionic surfactant system is positively charged under excess H_2S injected but no excess salt remains in solution. The final birefringent cationic/anionic surfactant $\text{L}\alpha$ -phase solutions consist of uni- and multilamellar vesicles. Both the original $\text{C}_{14}\text{DMAO}-\text{Zn}(\text{OOCCH}_2\text{C}_6\text{F}_{13})_2$ and the resulting catanionic $\text{C}_{14}\text{DMAOH}^+-\text{OOCCH}_2\text{C}_6\text{F}_{13}$ aqueous mixtures consist of uni- and multilamellar vesicles. The process is a novel and attractive assembly route is from metal-ligand complex to ionic vesicles. The purpose of the present study is to provide a new route for preparing novel materials using vesicle-phases constructed from organometallic ions. Vesicles formed of metal-ligand complexes converting to vesicles held together by ionic interactions play an important role in the construction of uni- and multilamellar vesicles as illustrated in Scheme 1.

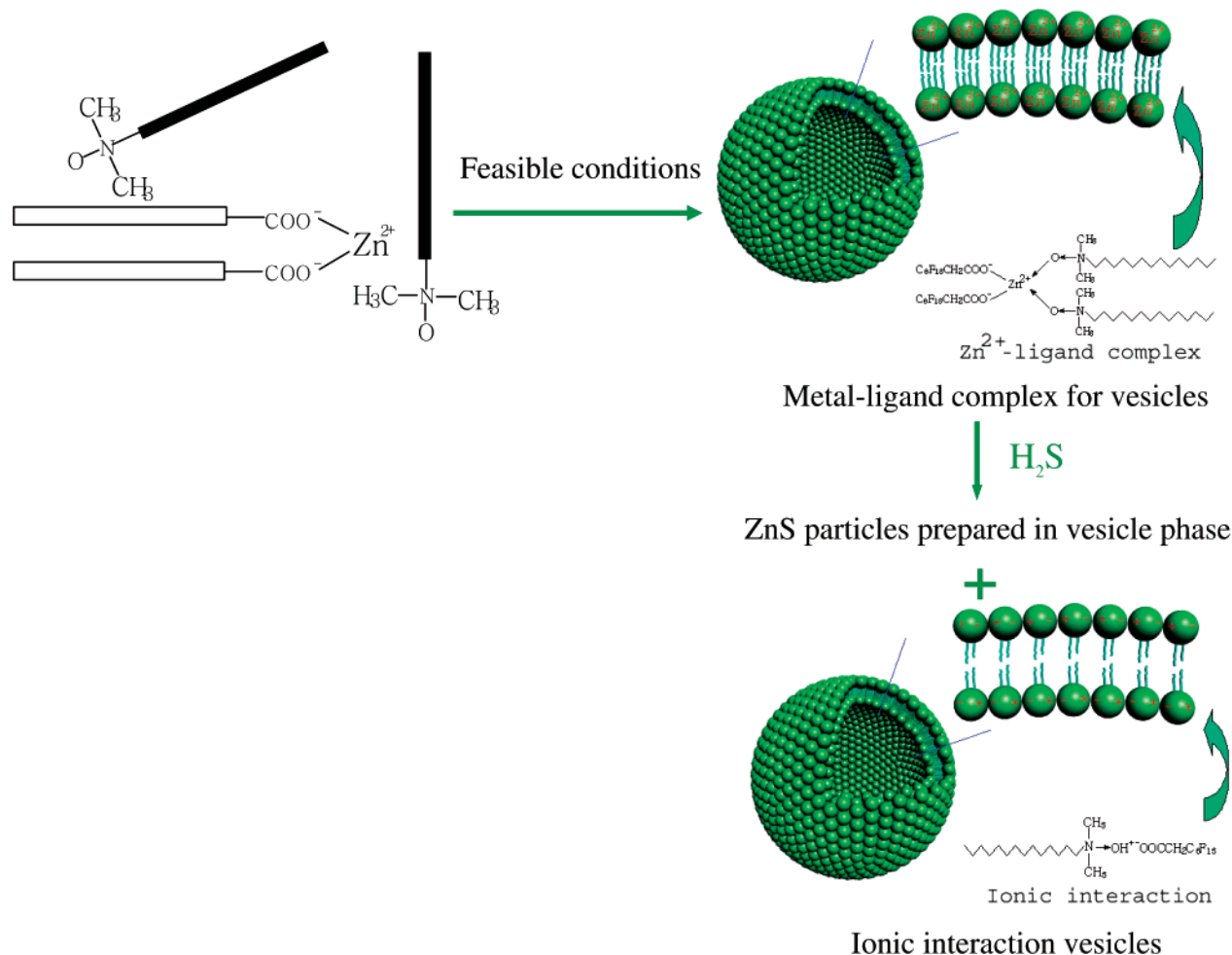
Experimental Section

Chemicals. Tetradecyldimethylamine oxide (C_{14}DMAO) was a gift from Clariant AG Gendorf (Frankfurt Am Main, Germany) and was delivered as a 25% solution. It was crystallized twice from acetone and characterized by melting point ($130.2-130.5^\circ\text{C}$) and $\text{cmc} = 1.4 \times 10^{-4} \text{ mol} \cdot \text{dm}^{-3}$. Zinc 2,2-dihydroperfluorooctanoate [$\text{Zn}(\text{OOCCH}_2\text{C}_6\text{F}_{13})_2$, purity $\geq 99\%$] was a gift from Hoechst-Gendorf (Frankfurt Am Main, Germany) and used without further purification. H_2S was prepared by the metathesis reaction ($\text{FeS} + 2\text{H}^+ \rightarrow \text{Fe}^{2+} + \text{H}_2\text{S}$) of FeS and dilute HCl in a Kipp 40-cm Gas Generator, and the gas flow rate was controlled.

Preparation of Birefringent $\text{L}\alpha$ -Phase of Uni- and Multilamellar Vesicles. Micelle solutions ($0.10 \text{ mol} \cdot \text{dm}^{-3}$ $\text{C}_{14}\text{-DMAO}$) were mixed with different amounts of $\text{Zn}(\text{OOCCH}_2\text{C}_6\text{F}_{13})_2$. The sample solutions were prepared at 75°C under stirring and then thermostated at 25°C after equilibrium for at least 4 weeks.^{16b} The sample solutions are thermodynamically stable up to a mole fraction $x_{\text{C}_6\text{F}_{13}\text{CH}_2\text{CCO}^-} = 0.395$. Between $x_{\text{C}_6\text{F}_{13}\text{CH}_2\text{COO}^-} = 0.20$ and 0.395 , a single transparent birefringent $\text{L}\alpha$ -phase which is very stable, turbid, and slightly bluish is observed. The phase boundaries were determined using conductivity measurements at $25.0 \pm 0.1^\circ\text{C}$.

Freeze-Fracture Transmission Electron Microscopy (FF-TEM) Observations. Birefringent $\text{L}\alpha$ -phase solutions were

SCHEME 1: A Transition Is Induced from Vesicles Composed of Metal–Ligand Complexes to Vesicles Held Together by Ionic Interactions, and ZnS Precipitates Are Prepared Inside the Vesicles^a



^a Only a bilayer vesicle model is shown, whereas multilamellar vesicles were observed in both the metal–ligand interaction and ionic interaction cases. A sector has been cut out for enhanced visibility. In the metal–ligand interaction case, Zn^{2+} is complexed to two CF-chains and two CH-chains (four chains). However, in the ionic interaction case, cationic ($\text{C}_{14}\text{DMAOH}^+$) and anionic ($\text{C}_6\text{F}_{13}\text{CH}_2\text{COO}^-$) surfactants construct the vesicle-phase (two chains).

characterized to determine the detailed structures by FF-TEM. One typical sample is viscoelastically birefringent $\text{L}\alpha$ -phase solution with $0.10 \text{ mol}\cdot\text{dm}^{-3}$ $\text{C}_{14}\text{DMAO}/0.022 \text{ mol}\cdot\text{dm}^{-3}$ $\text{Zn}(\text{OOCCH}_2\text{C}_6\text{F}_{13})_2$ ($x_{\text{C}_6\text{F}_{13}\text{CH}_2\text{COO}^-} = 0.31$). Another sample is the salt-free cationic/anionic system, $\text{C}_{14}\text{DMAOH}^+ \text{---} \text{OOCCH}_2\text{C}_6\text{F}_{13}$, where $\text{C}_{14}\text{DMAOH}^+$ was produced from C_{14}DMAO protonated with the H^+ ions released by H_2S and $\text{C}_6\text{F}_{13}\text{CH}_2\text{COO}^-$ was released from $\text{Zn}(\text{OOCCH}_2\text{C}_6\text{F}_{13})_2$ as Zn^{2+} was precipitated by H_2S . In this case, ZnS precipitates were removed by centrifugation and the solution was equilibrated for more than 4 weeks at 25°C .

A small amount of solution to be characterized was placed on a 0.1 mm thick copper disk covered with a second copper disk. The copper sandwich with the sample was frozen by plunging this sandwich into liquid propane which had been cooled by liquid nitrogen. Fracturing and replication were carried out at a temperature of -140°C . Pt/C was deposited at an angle of 45° . The replicas were examined in a CEM 902 electron microscope (Zeiss, Germany) operated at 80 kV.

Preparation and Characterization of ZnS Precipitates.

After 30 min the metathesis reaction ($\text{FeS} + 2\text{H}^+ \rightarrow \text{Fe}^{2+} + \text{H}_2\text{S}\uparrow$) started to flush out the impurity gases in the Kipp Generator, and H_2S gas was injected into a birefringent $\text{L}\alpha$ -phase solution with $0.10 \text{ mol}\cdot\text{dm}^{-3}$ $\text{C}_{14}\text{DMAO}/0.022 \text{ mol}\cdot\text{dm}^{-3}$

$\text{Zn}(\text{OOCCH}_2\text{C}_6\text{F}_{13})_2$ ($x_{\text{C}_6\text{F}_{13}\text{CH}_2\text{COO}^-} = 0.31$) at a controlled flow rate. The injection rate of H_2S gas into the birefringent $\text{L}\alpha$ -phase solution is key to the synthesis of ZnS precipitates. In the present synthesis, we controlled the flow rate to ~ 10 H_2S bubbles/min ($\sim 40 \mu\text{L}/\text{min}$). After 24 h, the H_2S gas flow was stopped but the sample solution was kept at room temperature for more than 10 days under air insulation to observe the changes. The resulting mixtures were centrifuged for 3 h at room temperature. The precipitates were characterized by X-ray diffraction (XRD) and X-ray photoelectron spectroscopy (XPS).

UV–vis spectroscopy measurements of the ZnS precipitates dispersed in vesicle-phase solution were carried out on a HITACHI UV–vis spectrophotometer (UV–vis 4100, Hitachi, Japan) operated at a resolution of 2 nm. The spectra were recorded using a quartz cuvette containing ZnS precipitates dispersed in vesicle solution but diluted with water.

ZnS particle crystal structure was characterized by X-ray diffraction (XRD), which was carried out on a Japan Rigaku diffractometer using Cu K α radiation ($\lambda = 1.54178 \text{ \AA}$) from a rotating anode X-ray generator operating at 50 kV and 200 mA. The electronic binding energy of ZnS was examined by X-ray photoelectron spectroscopy (XPS) using an ESCALab MKII instrument with Mg K α ($h\nu = 1253.6 \text{ eV}$). The binding energy

values obtained in the XPS analysis were corrected by referencing the C 1s peak at 284.60 eV.

For TEM measurements, a drop (4 μL) of the transparent saffron-colored viscoelastic solution of ZnS precipitates was placed on a carbon-coated, Formvar-covered TEM grid (copper grid, 3.02 mm, 200 mesh). The excess solution was wicked away with filter paper and the precipitates were dried at room temperature. The grids were examined using a JEOL 100CX-II TEM operating at 100 kV.

Results and Discussion

Vesicle-Phase of Metal–Ligand Complexes. C_{14}DMAO in water can form micelle solutions, which have a low viscosity. A $0.10 \text{ mol}\cdot\text{dm}^{-3}$ C_{14}DMAO aqueous solution has zero-shear viscosity, $|\eta^0| = 1.98 \times 10^{-3} \text{ Pas}$. The solubility of $\text{Zn}(\text{OOCCH}_2\text{C}_6\text{F}_{13})_2$ in water at room temperature is low because $\text{Zn}(\text{OOCCH}_2\text{C}_6\text{F}_{13})_2$ has a high Krafft point, $T_f = \sim 62.4^\circ\text{C}$, which makes for simple phase behavior. When C_{14}DMAO micelle solution was mixed with $\text{Zn}(\text{OOCCH}_2\text{C}_6\text{F}_{13})_2$, the phase behavior was very interesting. The Krafft temperature of $\text{Zn}(\text{OOCCH}_2\text{C}_6\text{F}_{13})_2$ is reduced when mixed with C_{14}DMAO micelle solution. For a $0.10 \text{ mol}\cdot\text{dm}^{-3}$ C_{14}DMAO micelle solution mixed with $\text{Zn}(\text{OOCCH}_2\text{C}_6\text{F}_{13})_2$, the $T_f = \sim 16.2^\circ\text{C}$ which was measured as the temperature at which a 0.1% (wt %) $\text{Zn}(\text{OOCCH}_2\text{C}_6\text{F}_{13})_2$ dispersion becomes clear on gradual heating. Even though a low Krafft point $\text{Zn}(\text{OOCCH}_2\text{C}_6\text{F}_{13})_2$ is induced by C_{14}DMAO micelle solutions, the samples were prepared at 75°C under stirring and then thermostated at 25°C .

For $0.10 \text{ mol}\cdot\text{dm}^{-3}$ C_{14}DMAO micelle solution mixed with increasing $\text{Zn}(\text{OOCCH}_2\text{C}_6\text{F}_{13})_2$ concentrations, the samples are thermodynamically stable up to a mole fraction $x_{\text{C}_6\text{F}_{13}\text{CH}_2\text{COO}^-} = 0.395$. From $x_{\text{C}_6\text{F}_{13}\text{CH}_2\text{COO}^-} = 0$ to 0.13, one can note a single transparent solution, which is the L_1 -phase. Between $x_{\text{C}_6\text{F}_{13}\text{CH}_2\text{COO}^-} = 0.13$ and almost 0.20 we observed macroscopic phase separation into a birefringent $\text{L}\alpha$ -phase on top of the L_1 -phase and an isotropic L_1 -phase at the bottom. After the two-phase region, from $x_{\text{C}_6\text{F}_{13}\text{CH}_2\text{COO}^-} = 0.20$ to 0.395, we observed a single transparent birefringent $\text{L}\alpha$ -phase that is very stable, slightly turbid, and bluish. The single transparent birefringent $\text{L}\alpha$ -phase contains uni- and multilamellar vesicles which were seen by FF-TEM observations. The samples with the mole fractions $x_{\text{C}_6\text{F}_{13}\text{CH}_2\text{COO}^-} > 0.395$ again separate into a two-phase $\text{L}_1/\text{L}_{\text{crystal}}$ -region. The upper phase is an isotropic L_1 -phase, and there are $\text{Zn}(\text{OOCCH}_2\text{C}_6\text{F}_{13})_2$ crystals at the bottom. One typically birefringent $\text{L}\alpha$ -phase sample with and without polarizers is shown in Figure 2a.

The Zn^{2+} -ligand complexes form vesicles in the aqueous mixtures of C_{14}DMAO and $\text{Zn}(\text{OOCCH}_2\text{C}_6\text{F}_{13})_2$. The vesicles may be the result of complexation between Zn^{2+} and the amine-oxide group of C_{14}DMAO . The vesicle-phase is ionically charged by Zn^{2+} but the ionically charges are not shielded because of the salt-free conditions, i.e., without counterions in the aqueous solutions. The complexation could be primarily demonstrated from the slightly blue and viscoelastic solutions formed when C_{14}DMAO solutions are mixed with $\text{Zn}(\text{OOCCH}_2\text{C}_6\text{F}_{13})_2$. To further examine the complexation between C_{14}DMAO and $\text{Zn}(\text{OOCCH}_2\text{C}_6\text{F}_{13})_2$, we prepared aqueous solutions of C_{14}DMAO and $\text{C}_6\text{F}_{13}\text{CH}_2\text{COOK}$. One sample of $0.10 \text{ mol}\cdot\text{dm}^{-3}$ $\text{C}_{14}\text{DMAO}/0.044 \text{ mol}\cdot\text{dm}^{-3}$ $\text{C}_6\text{F}_{13}\text{CH}_2\text{COOK}/\text{H}_2\text{O}$ ($x_{\text{C}_6\text{F}_{13}\text{CH}_2\text{COO}^-} = 0.31$) is shown in Figure 2b with and without polarizers. In Figure 2 (a and b), the two samples have the same mole fraction of $x_{\text{C}_6\text{F}_{13}\text{CH}_2\text{COO}^-}$ but have different metal-

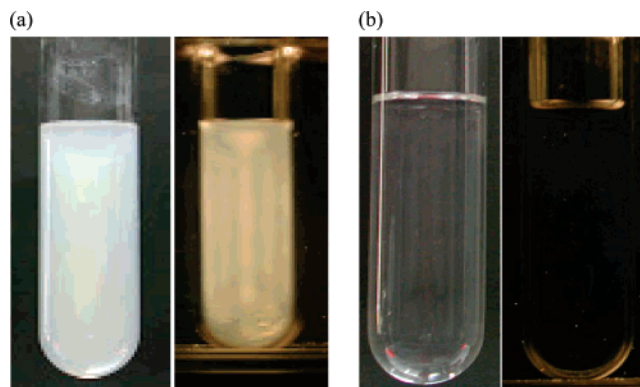


Figure 2. (a) Birefringent $\text{L}\alpha$ -phase of $0.10 \text{ mol}\cdot\text{dm}^{-3}$ $\text{C}_{14}\text{DMAO}/0.022 \text{ mol}\cdot\text{dm}^{-3}$ $\text{Zn}(\text{OOCCH}_2\text{C}_6\text{F}_{13})_2$, (b) L_1 -phase of $0.10 \text{ mol}\cdot\text{dm}^{-3}$ $\text{C}_{14}\text{DMAO}/0.044 \text{ mol}\cdot\text{dm}^{-3}$ $\text{C}_6\text{F}_{13}\text{CH}_2\text{COOK}$ (b). For both samples, $x_{\text{C}_6\text{F}_{13}\text{CH}_2\text{COO}^-} = 0.31$. Left sample without polarizers and right one with polarizers.

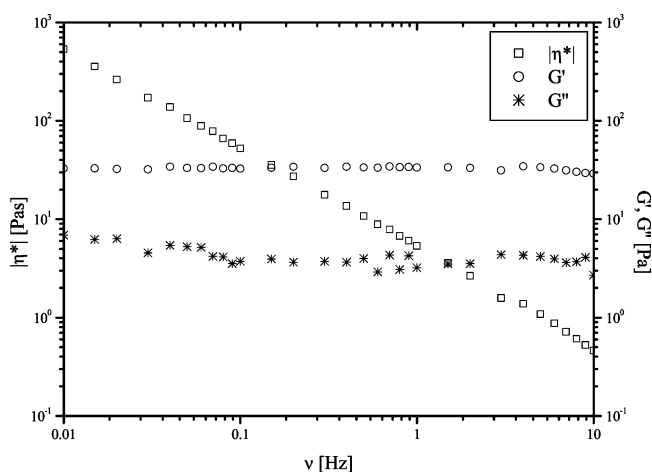


Figure 3. Rheogram of the oscillatory shear for one sample of $\text{L}\alpha$ -phase with $0.10 \text{ mol}\cdot\text{dm}^{-3}$ $\text{C}_{14}\text{DMAO}/0.022 \text{ mol}\cdot\text{dm}^{-3}$ $\text{Zn}(\text{OOCCH}_2\text{C}_6\text{F}_{13})_2$ ($x_{\text{C}_6\text{F}_{13}\text{CH}_2\text{COO}^-} = 0.31$) at 25°C .

see that the solution of C_{14}DMAO and $\text{Zn}(\text{OOCCH}_2\text{C}_6\text{F}_{13})_2$ is $\text{L}\alpha$ -phase with birefringence and in the aqueous mixtures of $\text{C}_{14}\text{DMAO}/\text{C}_6\text{F}_{13}\text{CH}_2\text{COOK}$ we only obtain only clear, isotropic, and low viscous or viscous L_1 -phase.

The birefringent $\text{L}\alpha$ -phase of C_{14}DMAO and $\text{Zn}(\text{OOCCH}_2\text{C}_6\text{F}_{13})_2$ mixtures has interesting rheological properties. It is highly viscoelastic and yield stress value so the solutions behave like Bingham fluids. In contrast, the rheological properties of the mixed surfactant solutions of C_{14}DMAO and $\text{Zn}(\text{OOCCH}_2\text{C}_6\text{F}_{13})_2$ are completely different from those of the $\text{C}_{14}\text{DMAO}/\text{C}_6\text{F}_{13}\text{CH}_2\text{COOK}$ mixtures, even though the mole fractions of $x_{\text{C}_6\text{F}_{13}\text{CH}_2\text{COO}^-}$ are the same in the two systems.^{16b} A typical rheogram of one $\text{L}\alpha$ -phase sample is shown in Figure 3. The rheogram of the $\text{L}\alpha$ -phase solution has the typical properties of multilamellar vesicles which behave in the same way as other charged multilamellar vesicle-phases with different compositions.^{16,19} One can see that both moduli are frequency independent, and the storage modulus ($G' = 33 \text{ Pa}$) is about 1 order of magnitude higher than the loss modulus ($G'' = 3.5 \text{ Pa}$).

The birefringent $\text{L}\alpha$ -phase in the $\text{C}_{14}\text{DMAO}/\text{Zn}(\text{OOCCH}_2\text{C}_6\text{F}_{13})_2/\text{H}_2\text{O}$ system consists of uni- and multilamellar vesicles which shown in Figure 4 (a–d). The features of the vesicles are apparent: (i) both uni- and multilamellar vesicles coexist; (ii) both uni- and multilamellar vesicles have polydisperse size distributions. The unilamellar vesicles have diameters ranging from about 40 nm to more than 500 nm, and the multilamellar

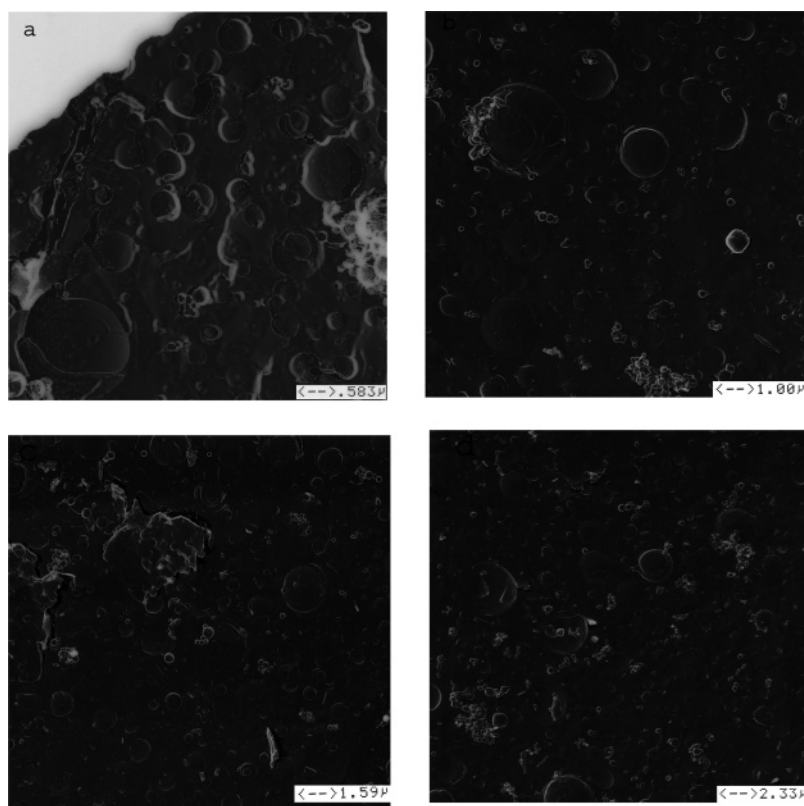


Figure 4. FF-TEM images of Uni- and multilamellar vesicles in $0.10 \text{ mol} \cdot \text{dm}^{-3} \text{ C}_{14}\text{DMAO}/0.022 \text{ mol} \cdot \text{dm}^{-3} \text{ Zn}(\text{OOCCH}_2\text{C}_6\text{F}_{13})_2$ aqueous mixtures. Bars correspond to different lengths (μm).

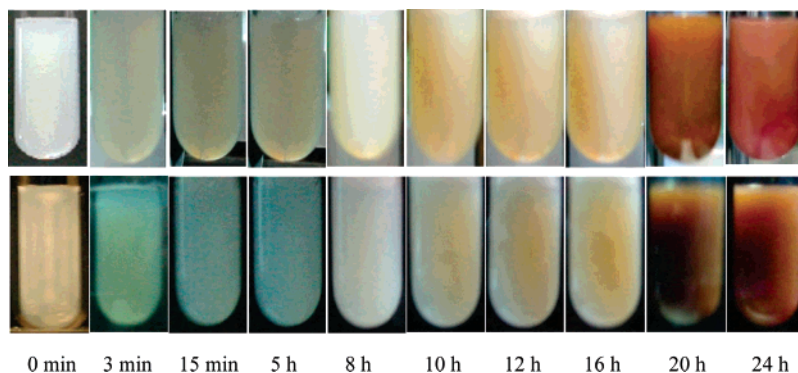


Figure 5. Color change of the birefringent $L\alpha$ -phase solution as H_2S gas was injected over time. Top without polarizers and below with polarizers.

vesicles have diameters ranging from about 500 nm to $3.0 \mu\text{m}$; (iii) the large unilamellar vesicles are relatively rare; (iv) in the multilamellar vesicles, the interlamellar spacing between two adjacent bilayers is about 40–80 nm.

Preparation of ZnS Precipitates and Vesicles Made from Ionic Interactions. The ionically charged vesicle-phase induced by Zn^{2+} –ligand complexation is not shielded because there are no counterions in the aqueous solutions. The vesicles have been prepared without introducing any additives such as cosurfactants. Such a vesicle-phase is important for many applications where a cosurfactant is not used. When H_2S gas was injected into the vesicle-phase, Zn^{2+} was precipitated by H_2S to produce semiconducting ZnS materials. The final solution after removing ZnS precipitates is a birefringent $L\alpha$ -phase with uni- and multilamellar vesicles as demonstrated by FF-TEM images. However, the components are cationic/anionic surfactants because the zwitterionic surfactant C_{14}DMAO is charged by the H^+ released from H_2S and then the combination cationic/anionic surfactant system $\text{C}_{14}\text{DMAOH}^+ - \text{OOCCH}_2\text{C}_6\text{F}_{13}$ forms. The

circulative vesicle formation during the preparation of ZnS precipitates by vesicle reproduction is novel.

An interesting result was the color change of the birefringent $L\alpha$ -phase solution over time as H_2S gas was injected (Figure 5). One can clearly see that the birefringent, slightly blue $L\alpha$ -phase solution was immediately changed after H_2S gas was injected immediately. Within 3 min after H_2S gas was injected, the solution was blue, but after 7 h it became ash-yellow-colored. After injecting H_2S for 18 h, a saffron-colored solution becomes a creamy mass by 24 h. We kept the final solution for 4 weeks and did not find any further change. The color change of the birefringent $L\alpha$ -phase should show the new materials produced by H_2S . The new products are certainly ZnS precipitates which are responsible for the color change of the solution. Duplicate observations were carried out to distinguish the time dependence and the concentration dependence of the color of the particles.

TEM experiments were carried out to characterize the ZnS precipitates. Figure 6 (a–f) displays the TEM images of the ZnS precipitates. Ring-shaped precipitates, rings with encap-

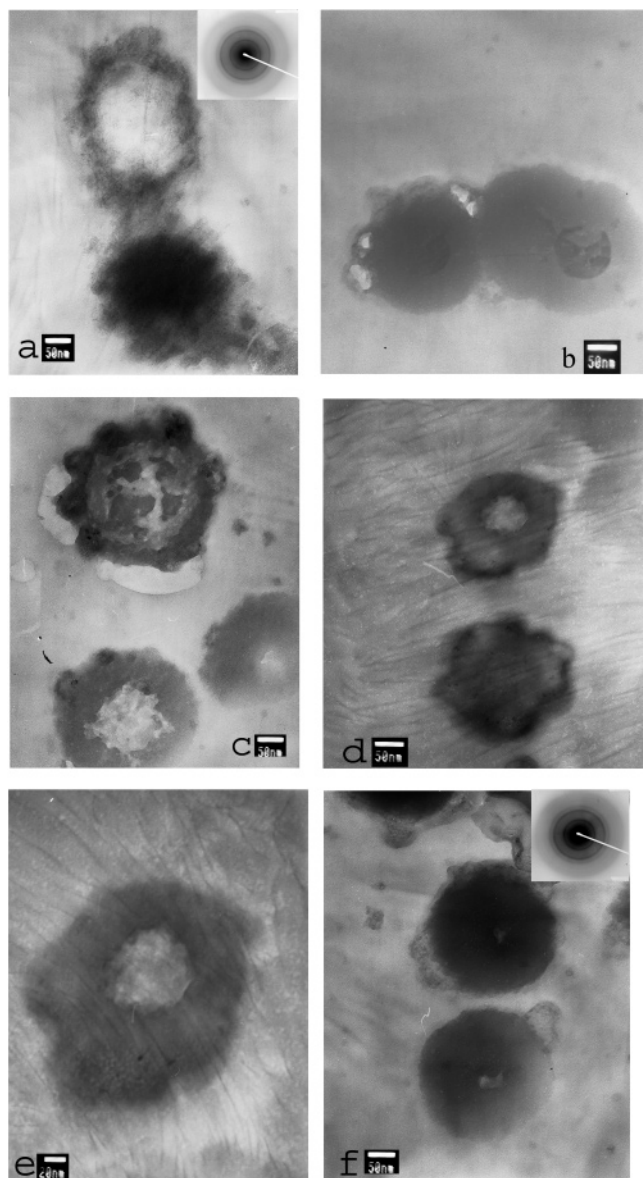


Figure 6. TEM images of ring structural ZnS materials with encapsulated central ZnS precipitates and regular spherical ZnS particles. Insets in Figure 6 (a and f) are the electron diffraction patterns.

sulated ZnS precipitates, and spherical associated ZnS particles were obtained. The electron diffraction patterns in Figure 6 (a and f) correspond to polycrystalline zinc-blende structures.²⁰

ZnS precipitates were characterized using UV–vis spectra on the mixtures of vesicle-phase with ZnS precipitates compared with spectra of the birefringent $L\alpha$ -phase solution. It is known that ZnS particles larger than about 6 nm (the size of an exciton in the bulk) start to absorb at a wavelength of about 337 nm. With decreasing particle size, the absorption peak shifts to shorter wavelengths as a result of quantum confinement effects. Figure 7 shows the UV–visible absorption spectra of the 1:5 (Figure 7a) and 1:50 (Figure 7b) solutions made by diluting the mixtures of vesicle-phase with ZnS precipitates with water and the birefringent $L\alpha$ -phase (Figure 7c). Considering that the birefringent $L\alpha$ -phase solution has no absorption in the observed wavelength at 260 nm (Figure 7c), the absorption peaks for 1:5 diluting solution at 260 nm are exclusively attributed to the ZnS nanoparticles. The UV spectra retain almost the same shape after the vesicle-phase with ZnS precipitates was diluted more than 50 times, indicating that ZnS precipitates were isolated as stable materials.

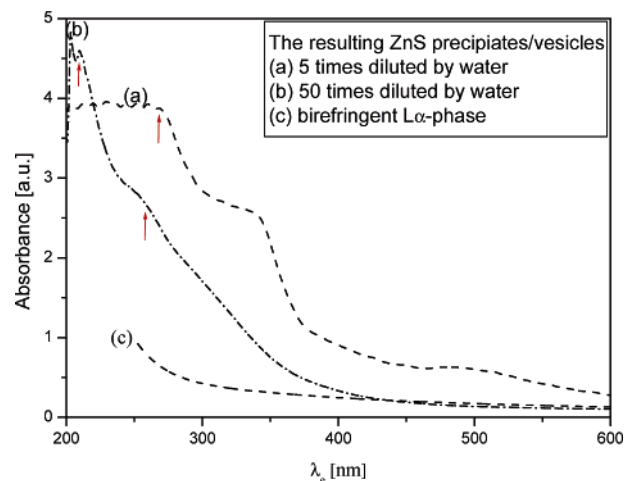


Figure 7. UV/visible spectra of the birefringent $L\alpha$ -phase solution and the vesicle-phase with ZnS precipitates diluted by water.

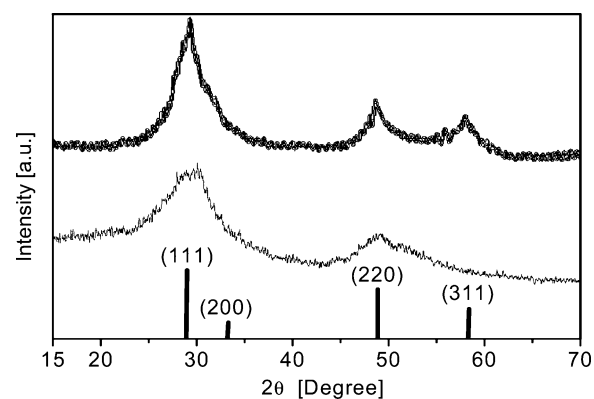


Figure 8. X-ray diffraction patterns for ZnS powders produced by sonochemical synthesis (upper curve), ZnS precipitates from the vesicle-template route (low curve), and the diffraction pattern of the zinc-blende crystal structure of ZnS (pillars).

To determine the nature of ZnS precipitates produced by the vesicle-template route, ZnS powders from two synthetic routes were analyzed by XRD. Ultrasound-induced colloidal ZnS²¹ was contrasted with the ZnS precipitates produced by vesicle-template route. The colloidal ZnS was prepared by the sonochemical synthesis, as described in great detail in the literature.²¹ In a typical synthesis of ZnS precipitates, $\text{Zn}(\text{ClO}_4)_2 \cdot 6\text{H}_2\text{O}$ (600 mg) and thioacetamide (200 mg) in 100 mL of distilled water are sonicated with a high-intensity ultrasonic horn at room temperature for 3 h. The ZnS precipitates from both routes were obtained by centrifugation, washed repeatedly with distilled water and ethanol, and then dried in a vacuum. X-ray diffraction patterns of ZnS powders produced from both methods are shown in Figure 8. For ZnS powders produced by sonochemical synthesis, the XRD pattern clearly shows the presence of broad peaks, corresponding to the zinc-blende crystalline structure. There are three diffraction peaks corresponding to the (111), (220), and (311) planes of the cubic crystalline ZnS. The domain size of the particles estimated from the Dybe–Scherrer formula ($D = \kappa\lambda/\beta \cos \theta$) is (1.4 ± 0.2) nm which is consistent with the results for the diameter of the sonochemistry-produced bare ZnS.²² For the ZnS precipitates formed by the vesicle-template route, the XRD diffraction profile is much broader and shows the presence of weak diffraction peaks. Two diffraction peaks correspond to the (111) and (220). However, the diffraction peak positions of ZnS precipitates match the ZnS crystal structure peaks and likely correspond with those of the zinc-blende structure. According to the characterization and the preparation

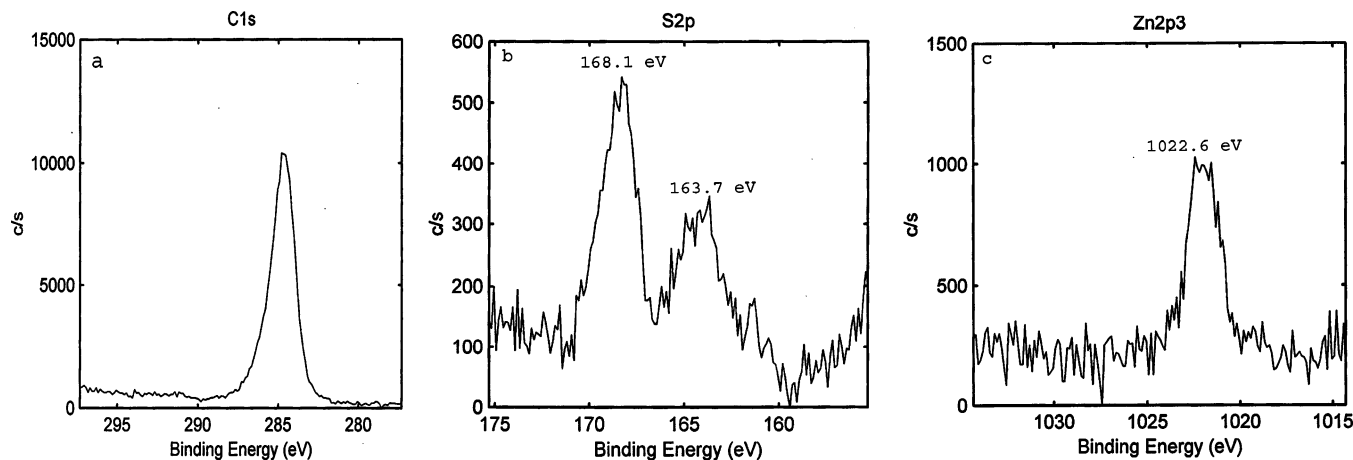


Figure 9. XPS spectra of ZnS precipitates: (a) C 1s spectrum, (b) S 2p spectrum, and (c) Zn 2p3 spectrum.

of ZnS precipitates by vesicle-template, we have isolated quantized (Q-) ZnS particles. The average diameters of the Q-ZnS particles were calculated using Scherrer's equation from the half width of the peak and found to be 1.6 ± 0.2 nm. The TEM observations for the ring-shaped semiconducting ZnS materials with encapsulated ZnS precipitates and associated ZnS particles in Figure 6 (a–f) show that they are constructed from the aggregation of ~ 1.6 nm ZnS crystallites.

The XPS spectra of ZnS precipitates produced by vesicle-template route are shown in Figure 9, including the C 1s (a), S 2p (b), and Zn 2p3 (c) spectra. One can obtain that the binding energy values of S 2p and Zn 2p3 are 163.7 and 1022.6 eV, respectively. The results are consistent with the binding energy values reported by Wagner.²³ The ratio of integral area for S 2p to ZnS 2p3 is calculated to be 1:1.086. The large peak with binding energy 168.1 eV might result from impurities such as CO₂, H₂O, and O₂ adsorbed on the surface of the ZnS precipitates.

Characterization of the Birefringent, Viscoelastic α -Phase Solution after Removing ZnS Precipitates. The birefringent, viscoelastic α -phase contains the cationic and anionic surfactants (C₆F₁₃CH₂COO[−] and C₁₄DMAOH⁺) because the C₁₄DMAO molecules are charged by the H⁺ released by H₂S. The macroproperties and structures of the cationic/anionic surfactant system were determined by rheological measurements and FF-TEM observations. Typical rheological properties of one sample with 0.10 mol·dm^{−3} C₁₄DMAO mixed with 0.022 mol·dm^{−3} Zn(OOCCH₂C₆F₁₃)₂ after removal of ZnS by centrifugation are shown in Figure 10. In comparison with the sample of α -phase with 0.10 mol·dm^{−3} C₁₄DMAO/0.022 mol·dm^{−3} Zn(OOCCH₂C₆F₁₃)₂ ($x_{\text{C}_6\text{F}_{13}\text{CH}_2\text{COO}^-} = 0.31$) (Figure 3), the rheological properties are essentially identical. The sample in Figure 10 has the same mole fractions of C₆F₁₃CHCOO[−] as in Figure 3. However, the system in Figure 10 is a cationic/anionic surfactant solution, and the static electronic interaction plays an important role in vesicle formation. The resulting cationic/anionic surfactant solution, which is similar to that in the C₁₄DMAO/C₆F₁₃CH₂COOH system, is a strongly birefringent α -phase.²⁴ The perfluoro-fatty acid protonates the zwitterionic surfactant because the pK_a of the perfluoro-fatty acid is smaller than that of C₁₄DMAO, and a cationic surfactant is formed that recombines with the anionic perfluorosurfactant formed by releasing a proton. The rheogram of the cationic/anionic surfactant α -phase solution is typical multilamellar vesicles which behave in the same way as the charged multilamellar vesicles in Figure 3. Both moduli are frequency

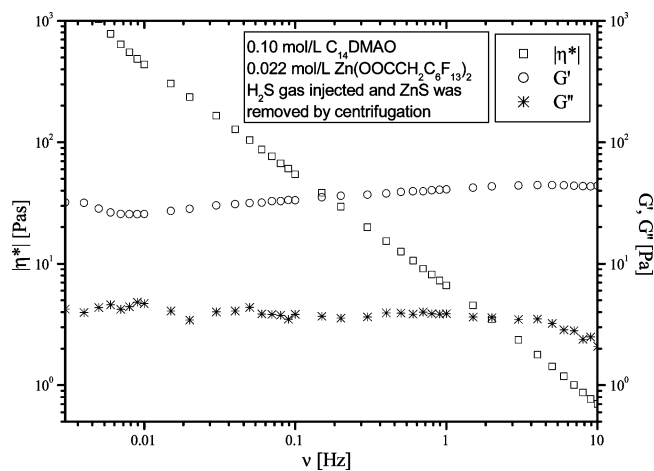


Figure 10. Rheogram of the oscillatory shear for one sample from 0.10 mol·dm^{−3} C₁₄DMAO/0.022 mol·dm^{−3} Zn(OOCCH₂C₆F₁₃)₂ solution after Zn²⁺ was precipitated by H₂S and ZnS was removed by centrifugation at 25 °C.

independent, and the storage modulus ($G' = 36$ Pa) is about 1 order of magnitude higher than the loss modulus ($G'' = 3.7$ Pa).

The birefringent α -phase in the cationic/anionic surfactant system, C₆F₁₃CH₂COO[−] and C₁₄DMAOH⁺, consists of uni- and multilamellar vesicles [Figure 11 (a–d)]. In comparison with the vesicle-phase formed by metal–ligand complexation in Figure 4 (a–d) and the salt-free vesicles of the C₁₄DMAO/C₆F₁₃CH₂COOH system observed in Figure 6 (a and b),²⁴ the features of the vesicles formed by the ionic interaction in the present system are similar but the components are different. One can observe that uni- and multilamellar vesicles coexist. Larger multilamellar vesicles, more than 2 μ m diameter, with many levels of encapsulation are present. From the FF-TEM images in Figure 11, one can see that the interlamellar spacing between the bilayers is rather compact and is in the range of 600 Å. The diameters of the unilamellar vesicles vary from about 10 nm to more than 2 μ m.

Uni- and multilamellar vesicle-phases were formed from metal–ligand complexation. The vesicles acted as stiff, independent microreactors since in the absence of salt and using a low-cvc (critical vesicle concentration) fluorinated component and a gaseous reactant, the contact making surfactant exchange does not occur during Brownian motion. Vesicle formation from ionic interactions crucially depends on the protonation of C₁₄DMAO to C₁₄DMAOH⁺, constructing a cationic surfactant system, C₁₄DMAOH⁺–OOCCH₂C₆F₁₃. To prove that this

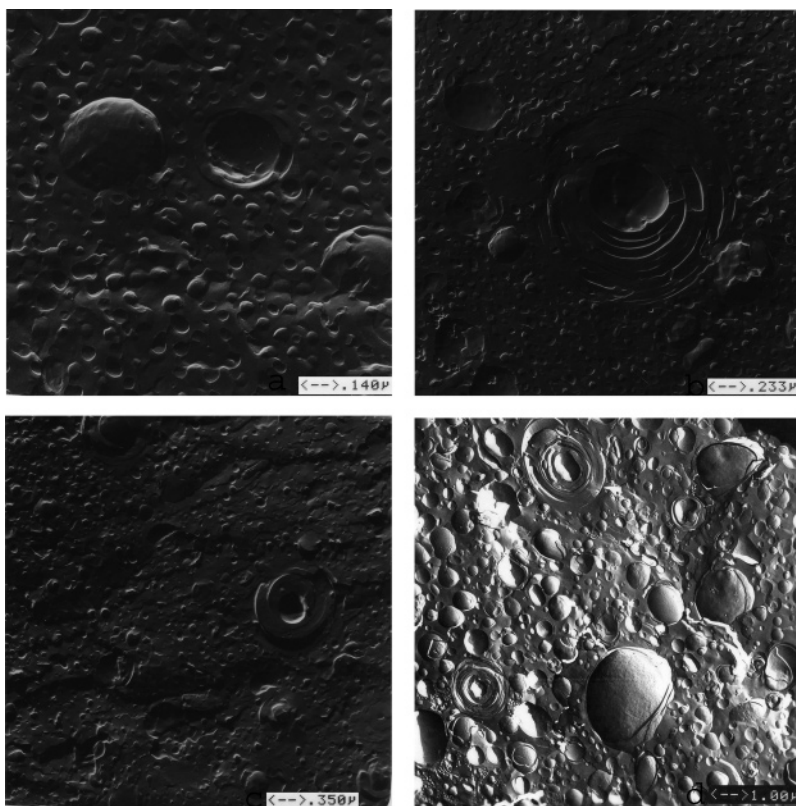


Figure 11. Freeze-fracture electron micrographs of one sample obtained from $0.10 \text{ mol} \cdot \text{dm}^{-3}$ $\text{C}_{14}\text{DMAO}/0.022 \text{ mol} \cdot \text{dm}^{-3}$ $\text{Zn}(\text{OOCCH}_2\text{C}_6\text{F}_{13})_2$ solution after Zn^{2+} was precipitated by H_2S and ZnS was removed by centrifugation. The sample was kept for more than 4 weeks for equilibrium at 25°C before the FF-TEM measurements.

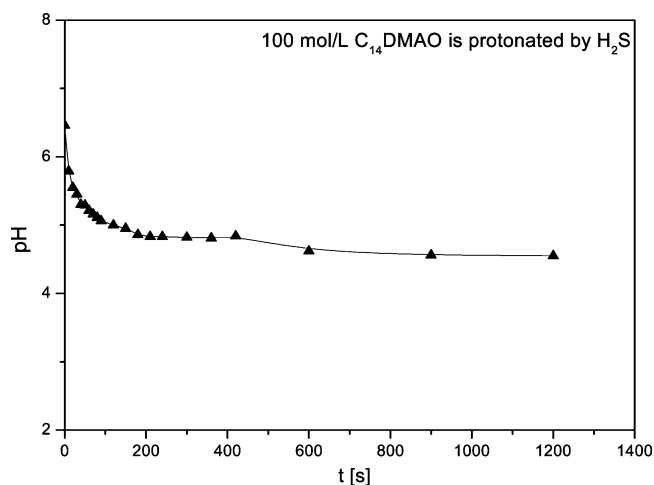


Figure 12. pH value change of $0.10 \text{ mol} \cdot \text{dm}^{-3}$ C_{14}DMAO micelle solution caused by H_2S injection.

transition from C_{14}DMAO to $\text{C}_{14}\text{DMAOH}^+$ occurs by reaction with the weak acid, we measured the pH values in $0.10 \text{ mol} \cdot \text{dm}^{-3}$ C_{14}DMAO micelle solution against the injection time of H_2S (Figure 12). From the measurements, one can see that the pH values of $0.10 \text{ mol} \cdot \text{dm}^{-3}$ C_{14}DMAO micelle solution with $\text{pH} = 6.46$ decrease rapidly once H_2S gas injection has begun. Approximately 200 s after H_2S gas was injected, the pH values reach equilibrium at $\text{pH} = 4.83$, indicating that the micellar solution was saturated with H_2S . In $\text{C}_{14}\text{DMAO}/0.022 \text{ mol} \cdot \text{dm}^{-3}$ $\text{Zn}(\text{OOCCH}_2\text{C}_6\text{F}_{13})_2$ vesicle solution, Zn^{2+} ions exist. After H_2S is injected into the vesicle-phase, the $\text{Zn}^{2+} + \text{H}_2\text{S} \rightarrow \text{ZnS} \downarrow + 2\text{H}^+$ reaction occurs, the H^+ ions are released, and C_{14}DMAO can be protonated more easily than that in C_{14}DMAO micelle solution, producing a truly catanionic surfactant system.

Conclusions

Two routes for production of vesicles, metal–ligand complexation and ionic interactions, have been described. In $\text{C}_{14}\text{DMAO}/\text{Zn}(\text{C}_6\text{F}_{13}\text{CH}_2\text{COO})_2$ aqueous mixtures, vesicle-phases can be obtained due to the complexation between the anionic surfactant with Zn^{2+} as counterion and the amine-oxide group of C_{14}DMAO . A salt-free cationic/anionic surfactant system, $\text{C}_{14}\text{DMAOH}^+ - \text{OOCCH}_2\text{C}_6\text{F}_{13}$, can be constructed by precipitating Zn^{2+} with H_2S . The ZnS precipitates with ring-shaped precipitates, rings with encapsulated ZnS precipitates, and spherical associated ZnS particles were obtained. This preparation route for novel vesicles and novel morphological materials is, to the best of our knowledge, reported for the first time. Furthermore, the simultaneous preparation of semiconductor materials during such vesicle formation opens up new avenues for preparation of materials with new morphologies and vesicle-phase reformation which can prevent the template from being destroyed during the preparation of particulates.

Acknowledgment. J. Hao and W. Liu gratefully acknowledge the support of this work by the NFSC (20473059, 20428101, 50421502), by the program of Hundreds of Talents of the Chinese Academy of Sciences (J. Hao), the Alexander von Humboldt Foundation, and the young-middle age Scientists' Awards (03BS083) and NFS, Shandong Province (Z2004B04) (J. Hao). The authors thank Dr. Pamela Holt (Shandong University) for assistance in preparation of the final manuscript.

References and Notes

- (1) Wang, W.; Efrima, S.; Regev, O. *J. Phys. Chem. B* **1999**, *103*(27), 5613–5621. (b) Zhang, Z.; Patel, R. C.; Kothari, R.; Johnson, C. P.; Friberg, S. E.; Aikens, P. A. *J. Phys. Chem. B* **2000**, *104*(6), 1176–1182. (c) Brinker, C. J.; Lu, Y.; Sellinger, A.; Fan, H. *Adv. Mater.* **1999**, *11*(7), 579–585. (d)

- Filankembo, A.; Pileni, M. P. *J. Phys. Chem. B* **2000**, *104*(25), 5865–5868. (e) Antonietti, M. *Curr. Opin. Colloid Interface Sci.* **2001**, *6*, 244–248.
- (2) Zhang, M.; Drechsler, M.; Müller, A. H. *Chem. Mater.* **2004**, *16*, 537–543. (b) Keller, S. L.; Boltenhagen, P.; Pine, D. J.; Zasadzinski, J. A. *Phys. Rev. Lett.* **1998**, *80*(2), 2725–2728.
- (3) Zemb, Th.; Dubois, M.; Demé, B.; Gulik-Krzywicki, Th. *Science* **1999**, *283*, 816–819.
- (4) Lee, B.; Luo, H.; Yuan, C. Y.; Lin, J. S. Dai, S. *Chem. Commun.* **2004**, 240–241.
- (5) Correa, N. M.; Zhang, H.; Schelly, Z. A. *J. Am. Chem. Soc.* **2000**, *122*, 6432–6434. (b) Pevzner, S.; Regev, O.; Lind, A.; Lindén, M. *J. Am. Chem. Soc.* **2003**, *125*, 652–653. (c) Zasadzinski, J. A.; Lisak, E.; Evans, C. *Curr. Opin. Colloid Interface Sci.* **2001**, *6*, 85–90. (d) Hubert, D. H. W.; Jung, M.; German, A. L. *Adv. Mater.* **2000**, *12*(17), 1291–1294. (e) Hubert, D. H. W.; Jung, M.; Frederik, P. M.; Bomans, H. H.; Meuldijk, J.; German, L. *Adv. Mater.* **2000**, *12*(17), 1286–1290. (f) Kisak, E. T.; Coldren, B.; Zasadzinski, J. A. *Langmuir* **2002**, *18*(1), 284–288.
- (6) Beck, R.; Abe, Y.; Terabayashi, T.; Hoffmann, H. *J. Phys. Chem. B* **2002**, *106*(13), 3335–3338. (b) Liu, T.; Burger, C.; Chu, B. *Prog. Polym. Sci.* **2003**, *28*, 5–26.
- (7) Pileni, M. P. *Nature Materials* **2003**, *2*, 145–150. Also see the references in this review article.
- (8) Israelachvili, J. N. *Intermolecular and surface forces*, 2nd ed.; Academic Press Ltd: New York, 1991.
- (9) Sijbesma, R. P.; Beijer, F. H.; Folmer, B. J. B.; Hirschberg, J. H. K. K. Lange, R. F. M.; Lowe, J. K. L.; Meijer, E. W. *Science* **1997**, *278*, 1601–1604. (b) Brunsveld, L.; Folmer, B. J. B.; Meijer, E. W.; Sijbesma, R. P. *Chem. Rev.* **2001**, *101*, 4071–4098. (c) Yamauchi, K.; Lizotte, J. R.; Hercules, D. M.; Vergne, M. J.; Long, T. E. *J. Am. Soc. Chem.* **2002**, *124*, 8599–8604.
- (10) Park, S.; Lim, J. H.; Chung, S. W.; Mirkin, C. A. *Science* **2004**, *303*, 348–351.
- (11) Hao, J.; Hoffmann, H. *Curr. Opin. Colloid Interface Sci.* **2004**, in press. Also see the references in this review.
- (12) Kaler, E. W.; Murthy, K. A.; Rodriguez, B. E.; Zasadzinski, J. A. *N. Science* **1989**, *245*, 1371–1374.
- (13) Jung, H. T.; Lee, S. Y.; Kaler, E. W.; Coldren, B.; Zasadzinski, J. A. *Proc. Natl. Acad. Sci.* **2002**, *99*, 15318–15322.
- (14) Dubois, M.; Demé, B.; Gulik-Krzywicki, Th.; Dediu, J. C.; Vautrin, C.; Désert, S.; Perez, E.; Zemb, Th. *Nature* **2001**, *411*, 672–675.
- (15) Hao, J.; Hoffmann, H.; Horbaschek, K. *J. Phys. Chem. B* **2000**, *104*, 10144–10153. (b) Hao, J.; Wang, J.; Liu, W.; Abdel-Rahem, R.; Hoffmann H. *J. Phys. Chem. B* **2004**, *108*, 1168–1172.
- (16) Jung, H. T.; Coldren, B.; Zasadzinski, J. A.; Iampietro, D. J.; Kaler, E. W. *Proc. Natl. Acad. Sci.* **2001**, *98*, 1353–1357.
- (17) Luo, X.; Li, C.; Liang, Y. *Chem. Comm.* **2000**, 2091–2092. (b) Ilhan, F.; Galow, T. H.; Gray, M.; Clabier, G.; Rotello, V. M. *J. Am. Soc. Chem.* **2000**, *122*, 5895–5896.
- (18) Knapp, R.; Schott, A.; Rehahn, M. *Macromolecules* **1996**, *29*, 478–480.
- (19) Hao, J.; Liu, W.; Xu, G.; Zheng, L. *Langmuir* **2003**, *19*, 10635–10640. (b) Horbaschek, K.; Hoffmann, H.; Thunig, C. *J. Colloid Interface Sci.* **1998**, *206*, 439–456.
- (20) Li, J.; Kessler, H.; Soulard, M.; Khouchaf, L.; Tuilier, M. H. *Adv. Mater.* **1998**, *10*, 946–949.
- (21) Sostaric, J. Z.; Caruso-Hubson, R. A.; Mulvaney, P.; Grieser, F. J. *Chem. Soc., Faraday Trans.* **1997**, *93*, 1791–1796.
- (22) Rossetti, R.; Hull, R.; Gibson, J. M.; Brus, L. E. *J. Chem. Phys.* **1985**, *82*, 552–559.
- (23) Wagner, C. D.; Riggs, W. W.; Davis, L. E.; Moulder, J. F.; Muilenberg, G. E. *Handbook of X-ray photoelectron spectroscopy*; Physical Electronics Division, Perkin-Elmer Corporation: Wellesley, MA, 1979.
- (24) Hao, J.; Hoffmann, H.; Horbaschek, K. *Langmuir* **2001**, *17*, 4151–4160.